INFRA-RED CCD SYSTEMS

C T Elliott*

ABSTRACT

A number of possible concepts for using IRCCDs in high performance thermal imagers are considered, ranging from a mirror-scanned block of devices to a large "staring" array. Possible technologies for fabricating the IRCCDs are reviewed including extrinsic silicon monoliths, silicon schottky barrier monoliths, InSb CIDs and CCDs, pyroelectric/Si hybrids and narrow-gap semiconductor/Si hybrids. Some emphasis has been given to the question of operating temperature and upper limits are estimated for each of the systems and technologies.

1. INTRODUCTION

The present generation of high performance thermal imaging systems employ detectors of semiconductor materials such as HgCdTe or InSb which are usually cooled to the temperature of liquid nitrogen (77K). The detectors are in the form of linear arrays or small two-dimensional arrays containing of order 100 elements. The elements are scanned over the image using mechanically driven mirrors in a parallel scan, serial scan or mixed serial/parallel scan mode.[1] Charge coupled devices have a useful role to play in these systems, either on or off the focal plane, in carrying out a multiplexing function for the parallel scan arrays, or a time delay integration function in the serial scan arrays.[2,3] However, in this paper we are concerned primarily with possible developments beyond the first generation systems and we anticipate that the most significant factor will be the integration of the detector with the signal processing circuitry on the focal plane, and the use of large scale integration technology to permit the use of very large numbers of detectors. We would expect some or all of the following system improvements to accrue:-

(a) A reduction in cost consequent upon the use of integrated circuit technology. Compare for example the predictions of very low cost CCD imagers in the visible.[4]

(b) A reduction in size and weight due to the simplification or complete avoidance of mechanical scanning, the use of fewer discrete electronic components and a simplified detector encapsulation.

(c) Improved performance resulting from the larger number of detectors used. The improved detector performance can also be used in other trade-offs eg to reduce the size of the optics.

(d) Reduced cooling requirements arising from

(i) the use of higher operating temperatures, made possible because the performance required of individual detectors is relaxed when large numbers are used

*Royal Signals and Radar Establishment, Malvern, England.

(ii) a reduction in cooling load because fewer wires are required between the cooled enclosure and ambient temperature.

Some possible system concepts employing large focal plane arrays are described below and possible technologies to fabricate the arrays are discussed. The operating temperature has important consequences for the cooling technology and the overall weight, size and power consumption of the system. Some emphasis is given to this question in comparing possible systems and technologies.

2. POSSIBLE SYSTEM CONCEPTS

2.1 In considering possible system concepts and fabrication technologies it is assumed that the future imager will be required to have a performance as good or better than that currently available with cooled linear arrays of detectors. We assume for the minimum specification: a noise equivalent temperature difference, NEΔT, in a 300K scene of 0.1K at zero range; a spatial resolution of 10^5 points over a two-dimensional field, and a frame rate of 25 Hz.

Some possible system concepts are illustrated schematically in figure 1.

2.2 In the "staring" array of fig 1(a) a detector is used for each point in the scene. The detectors are read out sequentially by on-chip signal processing and no mirror scanning is required. Such a system would represent the ideal, particularly if it could be operated without cooling. Two major problems exist in fabricating such a system; the high degree of uniformity required across the array and the large size of the chip, which could lead to a very low yield.

In order that fixed pattern noise in the display, due to D.C offsets on the detectors, should not obscure the temperature differences in the scene, we require the uniformity in the array to be of the order of the scene contrast.[2] For a 0.1K temperature difference in a 300K scene the contrast is 0.14% and 0.4% for the 8-14 μm and 3-5 μm windows respectively. This uniformity requirement refers to background limited detectors ie detectors in which the limiting noise is due to fluctuations in the background radiation from the 300K scene. For non-background limited detectors the uniformity requirements are very much more severe.[5] We may assume that, unless some sophisticated electronic uniformity correction is to be used, background limited performance is a necessary detector requirement. It should be noted however, that the quantum efficiency may be less than unity, the actual value required being determined by the required NEΔT of the imager.

The size of the chip required, assuming a 50 μm pitch for the detectors, is 1.5 cm by 1.5 cm. The technology for very large scale integration of this sort has been developed in silicon for visible imagers. In the author's view it is unlikely that the massive investment required to establish this technology in any other material will be forthcoming in the forseeable future.

2.3 One of the problems of the staring array, the non-uniformities arising from the D.C offsets, could, in principle at least be overcome by the use of a mechanical chopper to modulate the incoming radiation - a "blinking" array. A.C coupling at some point between the detector and the display would remove the D.C. offsets. This would necessarily introduce some additional complexity in the signal processing relative to a "staring" array.

2.4 The uniformity and fabrication problems can both be greatly reduced by retaining some mechanical scanning and using medium sized arrays (blocks) of, say, 32 x 32 elements. In the multi-block concept of Fig 1(b) an array of, say, ten blocks is parallel scanned across the scene with a "flapping" mirror to give a 320 line picture. The uniformity requirements are relaxed relative to a "staring" array because the detectors may be A.C coupled. Further relaxations in the uniformity requirements are obtained by using time-delay and integration in the direction of the scan.

2.5 Finally in figure 1(c) a single block scanned system is shown. The remarks on the multi-block scanned system apply here, except that a slightly more complicated scanning arrangement is required. The principal attraction of such a system, as we show below, may be in offering a performance similar to that of current high performance imagers but with much reduced detector cooling requirements.

3. POSSIBLE TECHNOLOGIES FOR IRCCD SYSTEMS

3.1 Table 1 shows a matrix of the four possible future systems concepts, described above, together with some possible technologies which might be used to fabricate them. In each column we give the detector figures of merit, M* and D*, for ideal quantum detectors operating with a peak response at 5 μm and 10 μm and also for a thermal detector, required to meet the systems performance as stated in section 2.1. (For a definition of M* and its relationship to D* see appendix 1). These are calculated from the thermal imaging equation

$$M^* = \frac{4F^2 B^{\frac{1}{2}}}{\Delta T t A_d^{\frac{1}{2}}}$$

where, F is the F/number of the system, assumed to be limited to F/2 for the staring, blinking and multi-block scanned arrays by optical aberration considerations and limited to F/1.5 for the single block scanned array by scanner design considerations; t is the transmission of the optics assumed to be 80%; ΔT is the noise equivalent temperature in the scene, assumed to be 0.1K, and A_d is the detector area, assumed to be $2.5 \times 10^{-5} cm^2$. The system bandwidth, B, is given by

$$B = \frac{Nf}{2n\eta_s}$$

where, N is the number of picture points, f is the frame rate, n is the number of elements and η_s is the scan efficiency. In scanned systems it is not usually possible to expose the detectors to the scene for more

than a fraction of the frame time. This fraction is known as the scan efficiency. We assume $\eta_s = 1$ for the "staring" array and 0.5 for all the other systems.

An estimate of the operating temperature required to achieve the required detector performance is given for each of the systems and each of the technologies. The way in which the figures were obtained is described below.

3.2 The Extrinsic Silicon Monolith

The attractions of an all-silicon approach to IRCCDs, which takes advantage of the highly developed MOS technology, are very great and the existence of large area arrays for visible imaging is an added encouragement. If the feasibility of the extrinsic silicon approach is established, production of the smaller block arrays might be expected to follow quite quickly. This technology and the silicon Schottky barriers appear to be the only ones which can be seriously considered for large, unscanned arrays at the present time.

When detecting visible light, with a photon energy greater than the band gap, an increase in both the majority and the minority carrier density is caused by the radiation. In order to detect far infra-red radiation, however, it is necessary to dope the silicon with an impurity having the appropriate ionization energy and in this case only majority carriers are generated by the radiation. The device configurations which can be used to detect and store the optically generated change are consequently different from those which can be used for visible imaging. One possible scheme has been described by Nummedal et al[6] and other possible schemes are discussed by Vere et al.[5]

There are a number of impurities which would produce a photo-response in the wavelength regions of interest. Some of these, together with their activation energies and solubility limits, are listed in table 2. The optimum activation energy depends on the detailed spectral dependence of the photo-ionization cross-section of the impurity and on the system requirements in terms of operating temperature, temperatures in the scene etc. We return to this point later and Logan[7] presents calculations of the activation energy required to obtain the maximum value of M*. Until very recently detailed photoconductive detector performance data had been published only for In and Ga. Pines and Baron[8] have reported background limited performance of Si:In detectors at temperatures up to about 60K in a background flux of $7 \times 10^{14} cm^2 s^{-1}$. The quantum efficiency was 50% and $D^*_{\lambda p}$ was 3×10^{11} cm $Hz^{\frac{1}{2}} W^{-1}$ Pines et al[9] report BLIP operation of Si:Ga devices at temperatures up to about 35K in a background flux of $1.1 \times 10^{17} cm^{-2} S^{-1}$. The operation of integrated detector/CCD structures in Si:Ga and Si:In, operating at temperatures below 20K has been demonstrated by Fraser et al[10] and Nummedal et al[6] in test arrays of up to 32 elements. The results indicate that a dynamic range in

excess of 80 dB can be achieved and that a relative transfer loss of less than 4×10^{-5} is possible when operating at low temperatures. A significant problem was that of optical cross talk between adjacent elements of the array. This arises primarily because the elements are relatively thick (about 500 μm) and are situated in convergent radiation which is reflected at the backside of the array. This type of problem is fundamental to the extrinsic detector approach because the photo-ionization cross sections of the dopants are small and relatively thick detectors are required to achieve adequate quantum efficiencies. The problem will be minimized by using high dopant densities in the silicon. For a further discussion see Vere et al.[5]

Although In and Ga are of interest for their relatively high solubility limits their activation energies appear to be far from optimum. Logan[7] indicates that, for the 8-14 μm band, E_A should be 0.12 in order to minimise M* for a 300K source and a dopant which has a photon capture cross-section like that predicted by Lucovsky.[11] This favours dopants like Te or Mg. Similarly for the 3-5 μm band activation energies corresponding to the short wavelength part of the band are indicated, favouring dopants such as Ni, S or Tl in preference to In.

It is indicated in section 2.1 and on table 2 that background limited operation is required for a "staring" array. It is also highly desirable for the block scanned array in order that the necessary performance can be achieved with the minimum detector thickness and cross-talk. For example, to obtain a $D^*_{\lambda p}$ at 5 μm of 7.5×10^{10} cm $Hz^{\frac{1}{2}}W^{-1}$, for a single block system, with detectors which are background limited in a 2π field of view, implies a quantum efficiency of 33%. Assuming a doping level of 5×10^{16} cm^{-3} and a photoionization cross-section of 2×10^{-16} cm^2, a sample thickness of about 400 μm would be required.

Elliott et al[12] have computed the temperature, T_{BLIP}, at which the optical carrier generation rate due to the background from a 300K scene, in a 2π field of view is equal to the thermal generation rate, for impurities with a Lucovsky photon capture cross-section. A plot of T_{BLIP} versus activation energy is shown in figure 2 for different values of the thermal capture cross-section, σ. Milnes[13] indicates that conventional dopants, with an attractive charge for the recapture of photo-carriers, have values of σ between 10^{-15} and 10^{-12} cm^2; neutral impurities have cross sections between about 10^{-17} and 10^{-15} cm^2, and repulsive centres can have cross-sections less than 10^{-22} cm^2. The plots are consistent with the observed behaviour of In and Ga assuming a cross-section of 10^{-12} cm^2. They also indicate that T_{BLIP} greater than 50K should be achievable in the 8-14 μm band and greater than 80K in the 3-5 μm band using dopants with similar value of σ but more optimized activation energies.

Sclar[14] has recently reported a detailed study of extrinsic Si detectors doped with a wide range of dopants for the two atmospheric bands. For the 8-14 μm range, background limited performance was obtained with Si:Al, Si:Ga and Si:Bi in a field of view of 30°, up to temperatures of the order 30K. Quantum efficiencies up to 35% were demonstrated. The detector Si:Mg, which should operate at higher temperatures, was limited by the presence of an extended spectral tail which was apparently associated with a low thermal activation energy of about 0.044 eV. For the 3-5 μm band, background limited performance (30°FOV) has been demonstrated for Si:In and Si:S up to temperatures of approximately 60K and 75K respectively. The results on Si:S are in good agreement with results recently obtained in our own laboratory and reported by Migliorato et al[15]. The detectivity as a function of temperature and the spectral response obtained by the latter are shown in fig 3 and fig 4.

It is of interest that the spectral response has a peak closer to the cut-off wavelength than that predicted by Lucovsky.[11] Sclar[14] indicates that this is generally true of donor impurities. It follows that n-type detectors should have better operating temperature characteristics than p-type devices.

It may be possible to obtain higher operating temperatures by using neutral or repulsive centres. An example of this type of centre, though at too short wavelength, is Si:Zn.[16] The author is not aware of any suitable dopants for the 8-14 μm band but a number of dopants are suggested by Elliott et al[12] for the 3-5 μm band. These include Hg, W, Pt and Ag counterdoped with shallow compensating centres. Very low capture cross-sections of $<10^{-17}cm^2$ have recently been measured in Si:Ag by Migliorato et al.[17] Another example of a counter-doped repulsive centre is the silicon divacancy which has been reported by Gross et al[18] to give good detector performance ($D^* = 3.7 \times 10^{11}$cm $Gz^{\frac{1}{2}}W^{-1}$). At 4 μm and at 77K.

3.3 Silicon Schottky Barriers

In order to operate as an infrared detector the Schottky barrier is illuminated through the silicon substrate causing internal photoemission from the metal into the silicon. The long wavelength and short wavelength cut-offs are determined by the Schottky barrier potential and the fundamental absorption of the silicon respectively. The great attraction of this device is its potential for good uniformity, because the quantum efficiency is independent of doping variations and lifetime variations in the semiconductor. Also the production of large area devices by depositing a metal onto a semiconductor is potentially a relatively cheap process.

The problem with this approach, from the point of view of high performance imagers, may be the low values of quantum efficiency which are available. Kohn et al[19] have reported Pd:p-Si detectors with a long

wavelength cut-off at 3.5 μm. They calculate that this system, with devices of area $2.8 \times 10^{-5} cm^2$ and with F/1 optics, would be capable of an NEΔT of 1.9°K. If, using alternative metals with lower work functions, the long wavelength cut-off could be extended to 4.5 μm or 5.5 μm they predict an NEΔT of 0.20K and 0.23K respectively. This assumes a non-uniformity of 1% in the quantum efficiency. If the fixed pattern noise due to non-uniformity could be avoided, the corresponding NEΔTs would be 0.15K and 0.04K.

The operating temperature of the device is determined by the need to reduce the dark current, due to thermal emission of electrons from the metal into the silicon, to an acceptable level. For $\lambda_c \leqslant$ 5 μm this means temperatures of about 80K.[19]

Kohn et al[19] have reported a 64 element linear array of detectors adjacent to a three phase charge coupled shift register. The approach used allows majority carriers to be read-out with depetion mode CCDs and incorporates background subtraction. Objects in the thermal scene at temperatures as low as 110C could be detected.

3.4 InSb CIDs or CCDs

The closest analogy to CID or CCD imaging in the visible with silicon devices, is infrared imaging using MIS structures in a narrow-gap semiconductor, whose intrinsic absorption matches the wavelength of interest. In this approach it is necessary to develop a dielectric technology for the narrow-gap semiconductor. The only material to have received significant attention to date is InSb, for which Kim[20] has reported MIS structures using silicon-oxynitride as an insulator and Thom et al[21] have used both alumina and silicon monoxide. Stable structures have been obtained with storage times greater than 0.1 Sec and with interface state densities of order $10^{11} cm^{-2}$. Very high dectivities up to 3.6×10^{12} cm $Hg^{\frac{1}{2}} W^{-1}$ have been obtained[20] for MIS sensors, in a background flux of $10^{13} cm^{-2} S^{-1}$. Thom et al[21] have measured a transfer efficiency of 0.9 for a four bit CCD with 200 μm bit length. An efficiency of 0.99 or better is predicted for shorter gate lengths.

It is unlikely that very high transfer efficiencies will be obtained in the near future and imager concepts[22] are mainly for block-scanned devices with the InSb operating in the CID mode and X-Y addressed with silicon circuits. Thom et al[21] suggest the use of InSb CCDs to perform a real time TDI function on a block array (~30 devices in the scan direction) where again very high transfer efficiencies would not be required.

The principal attractions of the monolithic InSb approach, relative to the extrinsic silicon, are the high optical absorption of the intrinsic material, which permits high quantum efficiencies without cross-talk, and the possibility of higher operating temperature. The temperatures

shown on table 1 were estimated on the assumption that the principal noise is shot noise on the dark current and that the detectivity, when the noise due to the background flux is negligible, is given by

$$D^*_\lambda = \frac{\eta e^{\frac{1}{2}}}{h\nu} \quad \frac{1}{(2J_D)^{\frac{1}{2}}}$$

The dark current, J_D, at 77K has been observed[20, 21] to be due to minority carrier generation in the space charge region. Assuming this to be true for all the temperatures of interest J_D is given by

$$J_D = \frac{en_iW}{2\tau_p}$$

Where n_i is the intrinsic carrier density assumed to be[23]

$$5.7 \times 10^{14}\ T^{3/2} \exp(-0.125/kT)$$

τ_p is the minority carrier lifetime assumed to be 0.1 μs and W is the depletion width. The latter was calculated as 2 μm assuming $N_D = 10^{15}cm^{-3}$, $\Delta\phi s$ = 2.5 V and the dielectric constant is 17. The temperature for the block-scanned and "blinking" arrays are shown in brackets since the criterion of obtaining adequate storage time outweighs that of obtaining adequate D* or M*. We estimate that a temperature of 80K is necessary in order that the storage time due to thermally generated currents should be long relative to a frame time.

3.5 Pyroelectric Detector / Si CCD Hybrid

Of the possible technologies considered here the pyroelectric/Si hybrid is unique in offering the prospect of uncooled operation (for a review of pyroelectrics see Putley[24]). Because of the differential nature of the pyroelectric response it is not applicable to a "staring" array but could be used in a "blinking" or scanned array. The detectivity obtainable from a good TGS single element detector exceeds by an order of magnitude the minimum value required for an NEΔT of 0.1K in a blinking array. However, there are two problems which can reduce the effective D*. One is the relatively low responsivity of the pyroelectric detector, which means that CCD noise will dominate in a directly coupled situation. Some gain is, therefore, required between the detector and the CCD. One indirect coupling possibility is described by Steckl et al.[25] The second problem can arise because of the heat sinking of the element at the interface with the silicon chip. For example with a 20 μm thick layer of TGS on silicon and with radiation modulated at 25 Hz, calculations[26] indicate that the signal is degraded by about a factor of 30. Logan suggests[26] that a simple solution may be to "chop" the radiation at 2.5 kHz, at which the thermal diffusion distance is about 10 μm and very little signal degradation would occur in a 20 μm thick layer.

It is unlikely that the required D* for 0.1K sensitivity in the block-scanned systems can be achieved. Part of the problem is the fall off in the performance of the pyroelectric devices with increasing frequency. We estimate the D* which might be obtained as follows. The value obtainable from the best single elements of TGS in 250 μm square size is about 5×10^{9} cm $Hz^{\frac{1}{2}}W^{-1}$ at a modulation frequency of 10 Hz. We assume that this D* can be maintained for a 50 μm square element size (ie stray capacitance is assumed to be negligible) and that there is no loss of D* on connecting to the CCD. The detector is required to operate at 4 kHz in the multi-block scanned array. Assuming D* varies af $f^{-\frac{1}{2}}$ the highest value we can expect is 2.5×10^{8} cm $Hz^{\frac{1}{2}}W^{-1}$ at 4 kHz. We therefore predict that the NEΔT will be greater than about 0.4K. Similarly for the single block NEΔT will be greater than about 2.5K.

NARROW GAP SEMICONDUCTOR DETECTOR/Si HYBRIDS

The concept here is to combine already developed high performance infrared detectors with Si CCDs. The problem is primarily one of making the interconnections with high yield. One approach is to mechanically interface blocks of detectors to align with contact pads on the silicon chip. Another might be to deposit the narrow-gap material epitaxially onto the silicon chip. The epitaxial approach is clearly an attractive one, but a survey of possible materials indicates potential problems in matching both the lattice parameter and the thermal expansion coefficient to the silicon values.

It seems unlikely that large "staring" or "blinking" arrays will be fabricated in the immediate future but the prospects for making 1000 element blocks, say, by mechanically interfacing are quite good. Such arrays could have important consequences either in improving the performance currently available from imagers cooled to 77K or in allowing the operating temperature to be raised, without loss of performance, to a level which is attainable with a simple cooler. Recent developments in reducing the power consumption of thermoelectric coolers make the latter prospect particularly appealing. Buist[27] has reported a cooler which can produce 193K with 33 mW of active load for 2 W input power (at 6 V). He also reports a 170K cooler which pumps 29 mW of active load for 10 W input power.

The operating temperatures shown in table 1 are estimated for photoconductive HgCdTe detectors with a peak response at 5 μm and at 10 μm. (The calculation was similar to that in reference (28) but with a revised value of the overlap integral, in the expression for Auger lifetime, of 0.3, which is more consistent with experimental data). A plot showing both calculated and experimental values of D^*_{λ} versus wavelength is given in fig 5. This is modified from reference (28) by the improved values for the Auger recombination and some more recent experimental data.[29] Other materials which might be considered for photoconductive detectors in the 3-5 μm band are III-V alloys such as InAsSb or GaInSb. The operating temperatures for photoconductive devices would be expected to be similar to those for HgCdTe. The bias

current levels and noise levels of photoconductive detectors are such that a pre-amplifier is required between the detector and the CCD. Grant et al[30] have reported the operation of a CCD processor with a bipolar pre-amplifier array at 77K. The amplifier gain was greater than 30 with a bandwidth of 1.8 MHz and good noise performance.

In some applications the low bias current of photodiodes may be an advantage in allowing direct coupling of the detector to the CCD.[25,31] Steckl and Koehler have made a theoretical analysis of HgCdTe diodes operating with CCDs at 77K in a delay-and-add mode for serial scan operation. They indicate that an NEΔT of 0.1K is possible. Steckl[32] has suggested recently that the use of heterostructures such as PbSnTe/PbTe would facilitate the construction of sandwich structures. The idea is to "invert" the heterostructure onto a silicon chip and to illuminate through the PbTe substrate. Full use is made of the detector active area and the detector can be handled prior to assembly on a relatively thick substrate. The injection efficiency of the PbSnTe/PbTe structure into a CCD has been calculated[32] and for a typical device an efficiency of 67% is calculated at 1.34 MHz, the minimum read frequency to avoid saturation of the CCD.

From the point of view of junction detectors operating at intermediate temperature, some of the best D* figures have recently been obtained by Holloway[33] on PbSeTe Schottky barriers. For example a D^*_λ at 5 μm, of 2.5×10^{10} cm $Hz^{\frac{1}{2}}W^{-1}$ was obtained at 190K and 6.3×10^{10} cm $Hz^{\frac{1}{2}}W^{-1}$ at 170K.

CONCLUSION

A number of possible system concepts employing IRCCDs and possible technologies for achieving them have been reviewed. The many potential advantages for systems, including reduced cost, reduced size and weight and higher operating temperatures, are such as to assure the future of the IRCCD. To predict which of the systems and which of the technologies will ultimately carry the day is impossible at this stage. The field is still open to innovation and invention, for example, in raising the operating temperature in extrinsic Si devices, in improving the sensitivity and extending the wavelength response of Schottky barriers or in developing a practical solution to the interface problem for hybrids. Also much will depend on developments in parallel technologies such as cooling engines and thermo-electric coolers.

ACKNOWLEDGEMENTS

The author whishes to express his thanks to his colleagues at RSRE for many helpful discussions; in particular Dr A W Vere, Dr P Migliorato, Dr E H Putley, Dr G Vanstone and Dr R M Logan. This work is published by permission of the Director, RSRE and the Copyright Controller HMSO.

APPENDIX 1

In order to compare the performance of detectors with different cut-off wavelengths for the detection of thermal radiation over finite atmospheric paths, the figure of merit M* has been defined as,[34, 35]

$$M^* (f, T_1, L) = D^* (\lambda_p, f, 1) \int_0^\infty R(\lambda)\, A(\lambda) \left(\frac{dW_\lambda}{dT}\right)_{T_1} d\lambda$$

where D* is measured at frequency f and normalised to 1 Hz bandwidth; $R(\lambda)$ is the spectral response of the detector, normalised to unity at the peak; $A(\lambda)$ is the atmospheric transmittance; W_λ is the spectral radiant emittance of the black body target, T_1 is the target temperature and L is the atmospheric range.

The M* values quoted in the text are at zero range. The table below gives values of M*(293K, 0 km)/D* (peak value for quantum detectors)

Detector	$M^*/D^*_{\lambda p}$
Ideal quantum detector, λ_c = 5 μm	1.5×10^{-5}
Ideal quantum detector, λ_c = 10 μm	1.8×10^{-4}
Thermal detector	5.7×10^{-4}

REFERENCES

1 See for example R F Anderson, Optical Engineering 13, 335-338, 1974.

2 D F Barbe, Proc IEEE 63, 38-62, 1975.

3 G F Vanstone "Time Delay and Integration Signal processing using CCDs" This conference.

4 R D Compton, Electro-Optic System Design p22, April 1974.

5 A W Vere "Monolithic-Extrinsic Silicon IRCCDs" This conference.

6 K Nummedal, J C Fraser, S C Su, R Baron and R M Finnila. Proceedings of the Int Conf on the Application of CCDs, p19, San Diego, 1975.

7 R M Logan "Calculation of Optimum Ionization Energy for Extrinsic Silicon Detectors" This conference.

8 M Y Pines and R Baron. Proceedings of the International Electron Devices p446, Meeting, Washington, 1974.

9 M Pines, D Murphy, D Alexander, R Baron and M Young. Proceedings of the International Electron Devices Meeting, p582, Washington, 1975.

10 J C Fraser, D H Alexander, R M Finnila and S C Su. The International Electronic Devices Meeting, Washington 1974.

11 G Locovsky, Solid State Comm 3, 299, 1965.

12 C T Elliott, P Migliorato and A W Vere. To be published.

13 A G Milnes "Deep Impurities in Semiconductors" p 93, John Wiley, 1973.

14 N Sclar, to be published Infra-red Physics, volume 16, 1976.

15 P Migliorato, A W Vere and C T Elliott. To be published in Applied Physics.

16 N R Mantena and E E Loebner, Proc Int Conf on Photoconductivity, Stanford, 1969, page 53. Ed EMPELL (Pergamon)

17 P Migliorato, C T Elliott and A W Vere to be published.

18 C Gross, R J Mattauch and T J Viola, J Appl. Phys 44, 735, 1973.

19 E S Kohn, S A Roosild, F D Shepherd and A C Yang, Int Conf on the applications of CCDs p59, San Diego 1975.

20 J C Kim, Proceedings of the International Conference on the Application of CCDs, p1, San Diego 1975.

21 R D Thom, R E Eck, J D Phillips and J B Scorso, Proc of the International Conference on the Application of CCDs p31, San Diego 1975.

22 A F Milton and M Hess. Proc of the Int Conf on the Applications of CCDs, p71, San Diego, 1975.

23 E H Putley "The Hall Effect and Semiconductor Physics" Dover, 1968 eds R K Willendson and A C Beer.

24 E H Putley "Semiconductors and Semimetals" eds R K Willardson and A C Beer V.5, p259, 1970.

25 A J Steckl, R D Nelson, B T French, R A Gudmundsen and D Schechter Proc. IEEE 63, 67, 1975.

26 R M Logan, RSRE, Malvern, Worcs, Private Communication.

27 R J Buist, IRIS Detector Speciality Meeting, California, 1974.

28 C T Elliott, M H Jervis and J B Phillips, Proceedings of Int Conference on the Physics of Narrow-Gap Semiconductors and Semimetals, Nice-Cardiff 1973

29 F D Morten, Mullard Ltd, Private Communication.

30 W Grant, R Balcerak, P Van Atta and J T Hall, Proc Int Conf on Applications of CCDs, p53, San Diego 1975.

31 A J Steckl and T Koehler, Proc Int Conf on Applications of CCDs, p247, San Diego 1973.

32 A J Steckl, Proc Int Conf on Applications of CCDs, p85, San Diego 1975.

33 H Holloway, Ford Motor Co, Durban, Michigan, Private Communication.

34 M H Jervis, Mullard Report 2048/R/0, 1970.

35 J W Sabey, Proc. Int Conf on Low Light and Thermal Imaging Systems, London, 1975.

TABLE 1 A matrix of system concepts and possible technologies with estimates of the operating temperature

	Staring Array Background Limited $M^*(293K,0Km) \geq 1.4 \times 10^5$			Blinking Array $M^*(293K,0Km) \geq 2 \times 10^5$			Multiblock Scanned $M^*(293K,0Km) \geq 6.3 \times 10^5$			Single block Scanned $M^*(293K,0Km) \geq 1.1 \times 10^6$		
	3-5μm $D^*_{\lambda p}=9.3\times10^9$	8-14μm $D^*_{\lambda p}=7.8\times10^8$	Thermal $D^*=2.5\times10^8$	3-5μm $D^*_{\lambda p}=1.3\times10^{10}$	8.14μm $D^*_{\lambda p}=1.1\times10^9$	Thermal $D^*=3.5\times10^8$	3-5μm $D^*_{\lambda p}=4.2\times10^{10}$	8-14μm $D^*_{\lambda p}=3.5\times10^9$	Thermal $D^*=1.1\times10^9$	3.5μm $D^*_{\lambda p}=7.5\times10^{10}$	8-14μm $D^*_{\lambda p}=6.3\times10^9$	Thermal $D^*=20\times10^9$
Extrinsic Silicon	80	50	—	80	50	—	80	50	—	80	50	—
Silicon Schottky barrier	80 $\Delta T>0.2K$	—	—	—	—	—	—	—	—	—	—	—
InSb CID or CCD	(190) 80	—	—	(180) 80	—	—	140	—	—	130	—	—
Pyroelectric/ Silicon hybrid	—	—	—	—	—	300	—	—	300 $\Delta T>0.4$	—	—	300 $\Delta T>2.5$
Narrow gap Semiconductor/ silicon	250	210	—	230	200	—	200	170	—	180	160	—

Table 2 Some possible impurities for extrinsic silicon detectors

Impurity a-acceptor d-donor	Activation Energy,(i) Optical,E_A (eV)	Cut-off Wavelength $1.24/E_A$ (μm)	Solubility cm^{-3}
Aℓ a	0.07	18	$2x10^{19}$ (ii)
Bi d	0.07	18	$8x10^{17}$ (ii)
Ga a	0.07	18	$3x10^{19}$ (ii)
Mg d	0.11	11	$>2x10^{15}$ (iii)
Te d	0.14	8.9	$\gtrsim 10^{19}$ (iv) $> 3x10^{16}$ (v)
In a	0.16	8.0	$2x10^{18}$ (vi)
S d	0.18	6.9	$3x10^{16}$ (ii)
Ni a	0.23	5.4	$6x10^{18}$ (vii)
Tℓ a	0.26	4.8	$> 10^{17}$ (viii)

(i) Ref 13
(ii) F A Trumbore Bell Syst Tech J 39, 205 1960
(iii) L T Ho and A L Ramdas Phys Lett A32A 23, 1970
Phys Rev 135, 462, 1972
(iv) T F Lee, R D Pashley, T C McGill and J W Mayer J App Phys 46, 391, 1975
(v) V P Prutken, A S Lyutovitch, M Yu Kardzhaubayev Krist Tonkikh Plenok p 145, 1970
(vi) S Fischler J Appl Phys 33 1615, 1962.
(vii) M Yashida and K Furusho Jap J Appl Phys 3,521, 1964
(viii) A M Smith "Fundamentals of Silicon Integrated Devices Technology (Ed R M Burger and R P Donovan) Vol 1 Prentice - Hall 1967

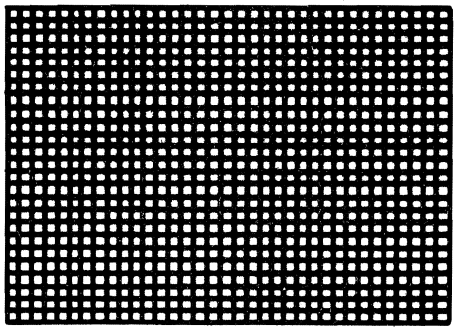

Fig Ia. A "staring" or "blinking" array with a detector for each picture point in the IR scene.

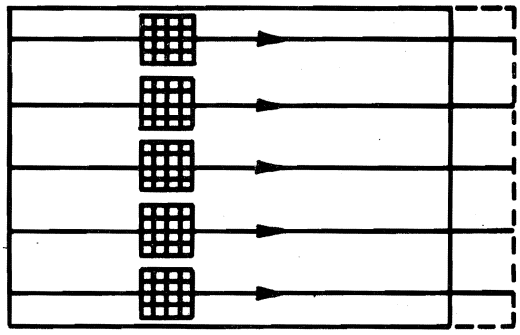

Fig Ib. Multiple blocks of detectors scanned over an image of the IR scene in a single sweep.

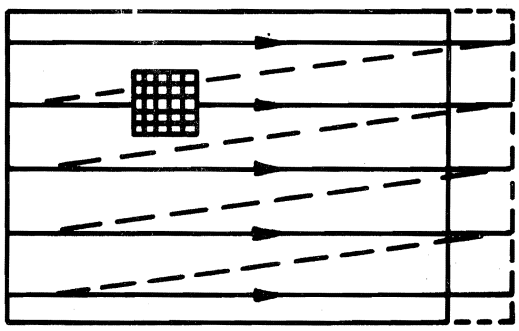

Fig Ic. A single block of detectors raster scanned over an image of the IR scene.

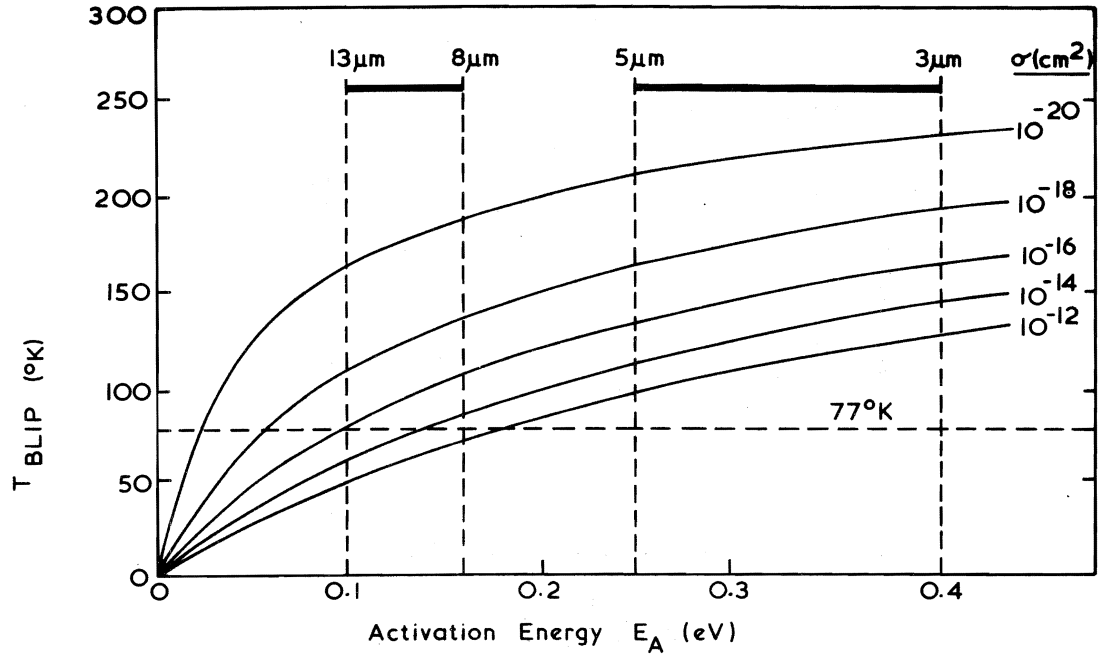

FIG. 2.

T_{BLIP} VERSUS IMPURITY IONISATION ENERGY, E_A, FOR EXTRINSIC SILICON PHOTOCONDUCTORS WITH DIFFERENT THERMAL CAPTURE CROSS-SECTIONS σ

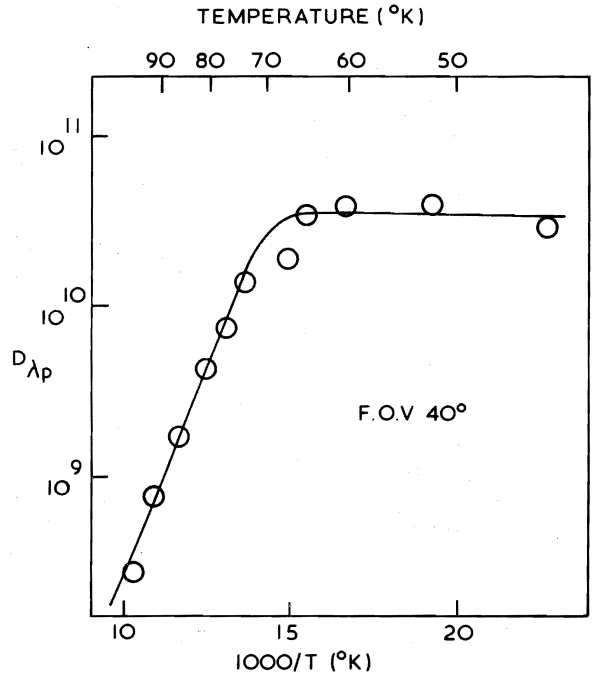

FIG. 3.

DETECTIVITY VERSUS RECIPROCAL TEMPERATURE FOR A Si:S DETECTOR WITH A 40° FIELD OF VIEW.

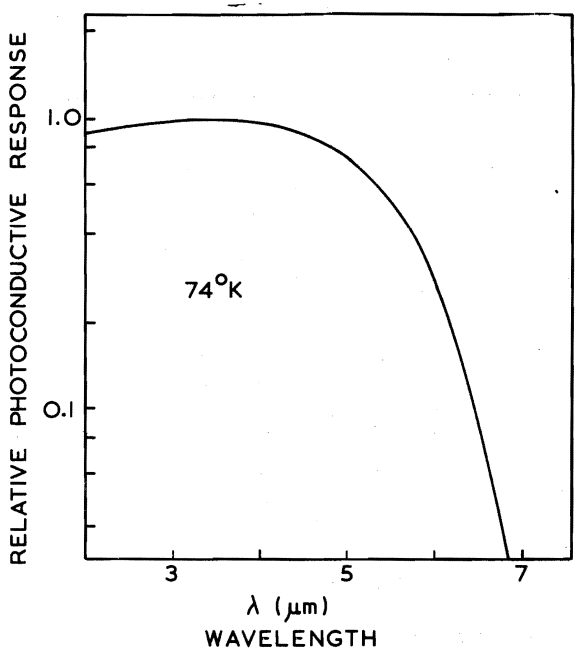

FIG. 4.

RELATIVE PHOTOCONDUCTIVE RESPONSE/INCIDENT PHOTON VERSUS WAVELENGTH FOR A Si:S DETECTOR AT 74 K

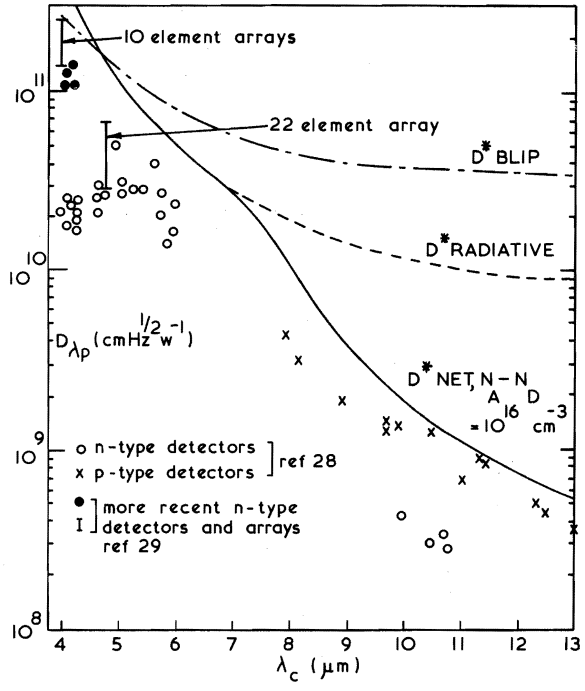

FIG. 5.

CALCULATED AND EXPERIMENTAL VALUES OF DETECTIVITY FOR 20 μm THICK PHOTOCONDUCTIVE CMT DETECTORS AT 193K, VERSUS CUT-OFF WAVELENGTH.